catalysts

MDPI

Article

Aerobic Oxidative Desulfurization of Liquid Fuel Catalyzed by P–Mo–V Heteropoly Acids in the Presence of Aldehyde

Reem Ghubayra [1,2], Rachel Hindle [2], Rana Yahya [3], Elena F. Kozhevnikova [2] and Ivan V. Kozhevnikov [2,*]

[1] Department of Chemistry, Faculty of Science, Jazan University, Jazan 45142, Saudi Arabia; rghubayra@jazanu.edu.sa
[2] Department of Chemistry, University of Liverpool, Liverpool L69 7ZD, UK; sgrhindl@student.liverpool.ac.uk (R.H.); efkozhev@liverpool.ac.uk (E.F.K.)
[3] Department of Chemistry, College of Science, University of Jeddah, Jeddah 23218, Saudi Arabia; ryahiya@uj.edu.sa
* Correspondence: kozhev@liverpool.ac.uk; Tel.: +44-151-794-2938

Abstract: Aerobic oxidative desulfurization (ODS) of model liquid fuel (dodecane spiked with dibenzothiophene (DBT)) was carried out in the presence of bulk and supported Keggin-type heteropoly acids $H_{3+n}PMo_{12-n}V_nO_{40}$ (HPA-n, n = 0–3) as heterogeneous catalysts and benzaldehyde as a sacrificial reductant. In the presence of bulk $H_4PMo_{11}VO_{40}$ (HPA-1), 100% of DBT was removed from fuel (converted to DBT sulfone) at 60 °C and ambient air pressure. Multiple catalyst reuse without loss of activity was demonstrated. The ODS reaction was strongly inhibited by radical scavengers. An unbranched radical chain mechanism was proposed.

Keywords: aerobic oxidative desulfurization; liquid fuel; dibenzothiophene; heteropoly acid; heterogeneous catalysis

Citation: Ghubayra, R.; Hindle, R.; Yahya, R.; Kozhevnikova, E.F.; Kozhevnikov, I.V. Aerobic Oxidative Desulfurization of Liquid Fuel Catalyzed by P–Mo–V Heteropoly Acids in the Presence of Aldehyde. *Catalysts* **2021**, *11*, 988. https://doi.org/10.3390/catal11080988

Academic Editors: Gilles Berhault, Hyun-Seog Roh and Salete Balula

Received: 8 July 2021
Accepted: 16 August 2021
Published: 18 August 2021

1. Introduction

Ultra-deep desulfurization of liquid fuels is an increasingly important task to meet stringent environmental regulations worldwide [1–3]. In particular, removing refractory aromatic sulfur compounds such as benzothiophenes, which are difficult to remove using conventional hydrodesulfurization (HDS) technology, is a major challenge [1,2]. In the past two decades, oxidative desulfurization (ODS) has been under development as a promising alternative/complementary technology for removing the refractory organosulfur compounds [4,5]. Typically, ODS is carried out using hydrogen peroxide as an oxidant (H_2O_2–ODS) in the presence of a catalyst under very mild conditions (50–70 °C, ambient pressure [4,5]; cf. 300–400 °C, 30–130 atm for HDS [1,2]), with organosulfur compounds oxidized to the corresponding sulfones. The use of dioxygen, preferably air, as the oxidant for ODS has attracted considerable attention as well, despite more forcing reaction conditions of O_2–ODS compared to H_2O_2–ODS (see recent reviews [6,7] and references therein). Polyoxometalates (POMs), especially Keggin-type POMs, are exceptionally active ODS catalysts for both H_2O_2–ODS [8–15] and O_2–ODS [6,7,16–20]. POMs have also been used as the catalysts for ODS with ozone [21]. The Keggin POMs include heteropoly anions $XM_{12}O_{40}^{m-}$, where M is the metal ion, typically Mo^{6+} and W^{6+}, and X is the central atom, most frequently P^{5+} and Si^{4+} [13,22]. These POMs are produced commercially as the corresponding heteropoly acids $H_mXM_{12}O_{40}$ (HPAs).

It has been reported that the addition of an aliphatic or aromatic aldehyde as a sacrificial reductant can greatly enhance the O_2–ODS of liquid fuel to remove benzothiophenes at reaction temperatures below 100 °C and ambient pressure [23–27]. Co(II) and Mn(II) salts [23,25] and POMs [24] have been reported as highly active homogeneous catalysts for the co-oxidation of benzothiophenes and aldehydes to produce the corresponding sulfones and carboxylic acids, which can be separated from fuel by solvent extraction and

adsorption with silica and alumina [23,24]. The major drawback of homogeneous ODS catalysts, however, is the difficulty of separating them from fuel; hence, in practical terms, heterogeneous catalysis would generally be preferred, even at the expense of catalytic activity.

The aldehyde-assisted ODS reaction is suggested to occur through radical chain co-oxidation of aldehyde and organosulfur compounds involving the formation of peroxy acid intermediate and its fast reaction with the organosulfur compound to give sulfone and carboxylic acid (Reactions (1) and (2)) [23,24]. Organic sulfides are well known as inhibitors of radical oxidation processes in liquid phase by interaction with hydroperoxides, similar to Reaction (2) [28].

$$RCHO + O_2 \rightarrow RCO_3H \quad (1)$$

$$2\ RCO_3H + R'_2S \rightarrow R'_2SO_2 + 2\ RCO_2H \quad (2)$$

The use of sacrificial reductants such as aldehydes, ketones, etc. for liquid-phase selective oxidation is an established technology that has been applied industrially, for example, for olefin epoxidation [28,29]. The benefit of aldehyde-assisted ODS over direct O_2–ODS is in the considerably milder reaction conditions (low temperature, ambient pressure and use of air instead of O_2), which would significantly improve process safety. The downside is the added cost of aldehyde and the necessity of removing the corresponding carboxylic acid from the treated fuel since the acidity of fuel (total acid number, TAN) is strictly regulated [30]. The aldehyde-assisted ODS makes a trade-off between aldehyde cost and ODS process safety. A wide range of aldehydes have been used efficiently in this reaction [6,7,23–25]. In practice, less expensive and amply supplied acetaldehyde can be applied [23]. The removal of carboxylic acid from the treated fuel can be achieved by extraction with aqueous Na_2CO_3 [23]. It should be noted that the use of direct O_2–ODS on real fuel (rather than a model fuel typically used in research) would inevitably cause co-oxidation of some fuel components to form organic oxygenates, including carboxylic acids, which would have to be separated like in the case of aldehyde-assisted ODS.

Here, we investigate the aldehyde-assisted aerobic ODS of model liquid fuel comprising dodecane spiked with dibenzothiophene (DBT) in the presence of benzaldehyde (PhCHO) as a model sacrificial reductant using bulk and supported Keggin-type mixed-addenda molybdovanadophosphoric heteropoly acids $H_{3+n}PMo_{12-n}V_nO_{40}$ (HPA-n, n = 0–3) as heterogeneous catalysts. PhCHO is chosen as a sacrificial reductant due to its fairly high reactivity and low volatility, allowing us to carry out the ODS reaction in a laboratory semi-batch reactor under air flow. HPA-n are well documented as catalysts for selective oxidation [13,31–33]. In particular, HPA-n with n = 2–6 are widely used as the catalysts for liquid-phase oxidation by O_2 [13,31–33]; their redox properties have been studied in detail ([13,33] and references therein). HPA-n possess a fairly high oxidation potential (~0.7 V vs. SHE), and their reduced forms can be re-oxidized by O_2; the latter occurs particularly easily for HPA-n with n = 2–6, probably via a multi-electron transfer mechanism [13,31–33]. It is V^{5+}/V^{4+} redox transformation within HPA-n that is responsible for the catalytic properties of HPA-n [13,33]. HPA-2 in conjunction with quaternary ammonium phase transfer agents (PTAs) has been reported as an active homogeneous catalyst for the O_2–ODS of model fuel (decalin + DBT) in the presence of isobutyraldehyde [24]. No attempt of recycling this catalyst has been made, however, which would be difficult to achieve in a homogeneous POM/PTA system. Here, we aim at developing an efficient and recyclable heterogeneous catalyst based on HPA-n for aldehyde-assisted aerobic ODS and gaining mechanistic insights into this reaction.

2. Results and Discussion

Heteropoly anions in all HPA-n catalysts studied, including bulk HPA-n and their Cs and Na salts, as well as HPA-1 supported on silica and activated carbon, had the Keggin structure, as confirmed by DRIFT spectroscopy, which is extensively used for fingerprinting purposes and structural elucidation of POMs [22]. The DRIFT spectra of the bulk catalysts

(Figure 1) exhibit four characteristic IR bands of P–O, M = O, M–O–M (corner-sharing) and M–O–M (edge-sharing) groups from 1100–700 cm^{-1}, for example, for HPA-1, at 1063, 964, 866 and 786 cm^{-1}, respectively, in agreement with the literature [34,35]. DRIFT spectra for 15%HPA-1/C (Figure S1, Supplementary Materials) and 15%HPA-1/SiO_2 (Figure S2) show the same bands of HPA-1. The XRD pattern for bulk crystalline HPA-1 (Figure 2) is in agreement with the literature [36]. No HPA-1 crystal phase is observed in supported catalysts 15%HPA-1/SiO_2 and 15%HPA-1/C (Figure 2), which indicates a fine dispersion of HPA-1 on the surface of supports. Bulk HPA-n have small surface areas, 2–15 m^2g^{-1} (Table 1), typical of bulk HPAs [13].

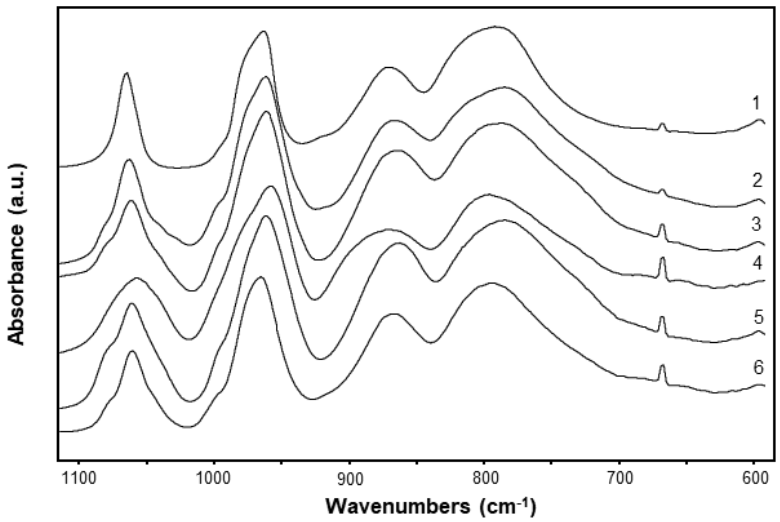

Figure 1. DRIFT spectra of HPA-n (powdered in KBr): HPA-0 (**1**), HPA-1 (**2**), HPA-2 (**3**), HPA-3 (**4**), Na-HPA-2 (**5**) and Cs-HPA-1 (**6**).

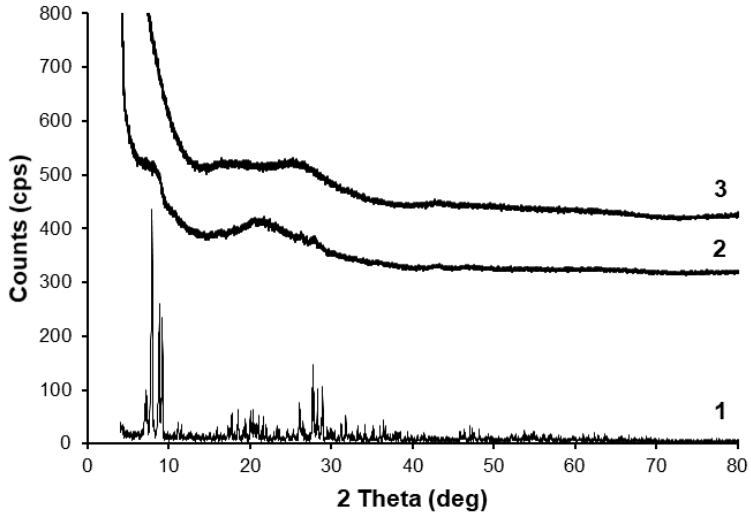

Figure 2. XRD patterns (CuKα radiation, λ = 1.542 Å) for bulk HPA-1 (**1**), 15%HPA-1/SiO_2 (**2**) and 15%HPA-1/C (**3**).

Table 1. Information about catalysts.

Catalyst	H_2O [1] (wt%)	S_{BET} [2] (m^2g^{-1})	Pore Volume [3] (cm^3g^{-1})	Pore Diameter [4] (Å)
HPA-0	13.5	14.8	0.018	48
HPA-1	12.3	15.5	0.020	52
HPA-2	12.8	2.4	0.0044	72
HPA-3	12.0	2.6	0.0060	93
Cs-HPA-1	5.2	8.9	0.15	67
Na-HPA-2	13.0	1.7	0.0046	106
15%HPA-1/SiO_2		236	1.29	219
15%HPA-1/C		928	0.81	35

[1] Water of crystallization from TGA in the temperature range of 40–250 °C. [2] BET surface area; HPA samples pre-treated at 150 °C/1 Pa. [3] Single point pore total volume. [4] Average BET pore diameter.

Figure 3 shows the results of initial screening of all bulk HPA-n catalysts in the aerobic ODS at 60 °C and a PhCHO/DBT molar ratio of 12. As can be seen, the V-containing HPA-n (n = 1–3) and their Cs and Na salts exhibit significantly higher activity (89–95% DBT conversion) than the V-free HPA-0 (41% DBT conversion), which can be explained by the lower oxidation potential of HPA-0 [13]. Reaction products were DBT sulfone and benzoic acid (from GC and FTIR analysis). The sulfone, insoluble in dodecane, precipitated out. The results indicate that the acidity of HPA-n does not play any significant role since the activity of the Cs and Na salts was close to that of HPA-n. Among the catalysts tested, HPA-1 and HPA-3 had a higher catalytic activity (95% DBT conversion). For further testing, the HPA-1 was chosen to minimize the amount of V in the catalyst. It has been reported that substitution of one V^{5+} for Mo^{6+} in $H_3PMo_{12}O_{40}$ increases the thermal stability of HPA, however, the stability decreases upon further substitution [13], making HPA-1 the most stable compound among HPA-n. Regarding the redox properties, HPA-1 is a one-electron oxidant due to reduction of V^{5+} to V^{4+} in the heteropoly anion with an oxidation potential of ~0.7 V (vs. SHE) [13]: $[PMo_{12}V^{5+}O_{40}]^{4-} + e^- \rightarrow [PMo_{12}V^{4+}O_{40}]^{5-}$.

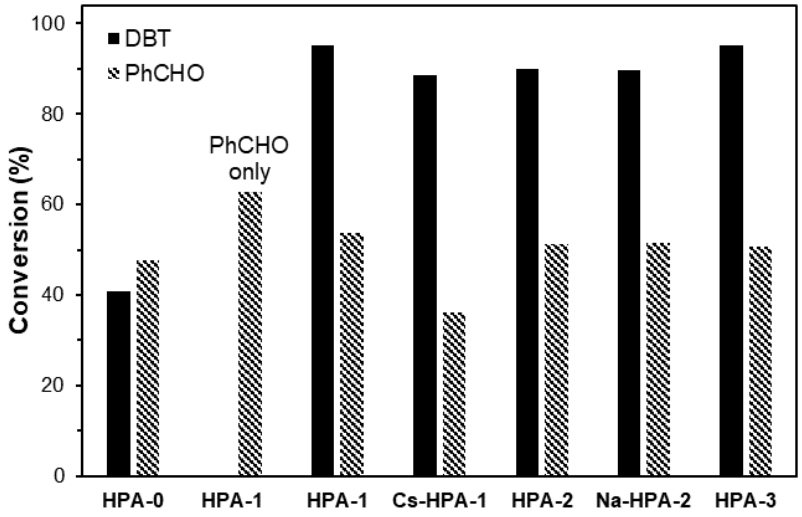

Figure 3. Effect of HPA-n catalyst (0.10 g, 0.04–0.05 mmol) on aerobic oxidation of DBT (0.40 mmol) in the presence of PhCHO (4.9 mmol) at 60 °C, 10 mL dodecane solvent, 20 mL min^{-1} air flow, 1300 rpm stirring speed and 2 h reaction time.

Table 2 shows the representative results on aerobic co-oxidation of DBT (0.50 mmol) and PhCHO (0–5.9 mmol, PhCHO/DBT = 0–12 mol/mol) in dodecane (10 mL) in the presence of bulk HPA-1 (0.10 g, 0.048 mmol) at 40–100 °C under air flow (20 mL min^{-1}, bubbling through the reaction mixture at ambient pressure) and 1300 rpm stirring speed.

Every reaction was repeated at least twice with a good reproducibility (see Section 3.3). In the absence of DBT, benzoic aldehyde was readily oxidized to benzoic acid (entry 1), whereas no DBT oxidation occurred in the absence of PhCHO (entry 2). The reaction did not depend on the rate of air flow, which varied from 10 to 30 mL min^{-1}. The use of pure O_2 instead of air did not affect the reaction either (cf. entries 6 and 16). This indicates sufficient oxygen supply as required for efficient radical chain propagation [28] (see below).

Table 2. Aerobic co-oxidation of DBT and PhCHO catalyzed by HPA-1 [1].

Entry	DBT (mmol)	PhCHO (mmol)	Temperature (°C)	Time	Conversion (%)	
				(h)	DBT	PhCHO
1	0	4.9	60	2.0	-	63
2	0.50	0	60	2.0	0	0
3	0.50	1.0	60	2.0	1.6	11
4	0.50	2.0	60	2.0	23	27
5	0.50	2.9	60	2.0	31	30
6	0.50	4.9	60	2.0	86	50
7	0.50	5.9	60	2.0	100 [2]	63
8 [3]	0.50	5.9	60	2.0	10	42
9 [4]	0.50	5.9	60	2.0	14	26
10	0.50	4.9	40	2.0	18	28
11	0.50	4.9	80	2.0	93	71
12	0.50	4.9	100	1.2	100 [2]	75
13	0.50	1.8	100	2.0	55	64
14	0.50	2.8	100	2.0	100 [2]	77
15	0.50	3.7	100	1.3	100 [2]	69
16 [5]	0.50	4.9	60	2.0	84	53

[1] 0.10 g catalyst (0.048 mmol HPA-1), 10 mL dodecane, 20 mL min^{-1} air flow rate, 1300 rpm stirring speed. [2] The amount of DBT after reaction below detection limit of FID detector. [3] 3.0 mmol of 1,4-benzoquinone added. [4] 3.0 mmol of 2,6-di-tert-butyl-4-methylphenol added. [5] Pure O_2 instead of air used (cf. entry 6).

The efficiency of the ODS reaction was greatly dependent on the PhCHO/DBT ratio. Thus, when increasing the PhCHO/DBT molar ratio from 1 to 12, the DBT conversion at 60 °C increased from 1.6 to 100% (Table 2, entries 3–7). A similar effect has been observed with homogeneous Co(II) catalyst [23]. Reaction temperature had also a strong effect on DBT conversion, which increased five-fold from 18 to 100% when increasing the temperature from 40 to 100 °C (entries 10–12).

The ODS reaction was strongly inhibited by chain-breaking radical scavengers such as 1,4-benzoquinone and 2,6-di-tert-butyl-4-methylphenol [28] (cf. entry 7 and entries 8 and 9, Table 2). This supports the radical chain mechanism suggested in previous reports [23,24].

From the results presented in Table 2, the aldehyde-assisted aerobic ODS with bulk HPA-1 as a heterogeneous catalyst allowed removing 100% DBT from the model fuel in a 2 h reaction time either at 60 °C and PhCHO/DBT = 12 mol/mol (entry 7) or at 100 °C and PhCHO/DBT = 5.6 (entry 14). As expected, the truly homogeneous $Co(OAc)_2$ catalyst has a higher activity, removing >99% DBT in 45 min at 40 °C and PhCHO/DBT = 4 mol/mol with pure O_2 as the oxidant at 1 bar pressure [23]. However, the Co(II) catalyst has the drawback of being non-recyclable. On the other hand, a non-recyclable homogeneous HPA-2/TPA catalyst in emulsion biphasic system MeCN–decalin also removes >99% DBT in 4 h at 60 °C and isobutyraldehyde/DBT = 10 with pure O_2 as the oxidant [24], hence showing a comparable activity to the bulk HPA-1 catalyst.

In contrast to the above homogeneous catalysts, the bulk HPA-1 catalyst exhibited excellent recyclability, as illustrated in Figure 4. It withstood multiple reuses without loss of its activity in five consecutive runs. No catalyst leaching was detected by ICP–OES analysis of post-reaction liquid phase. This is not unexpected since HPA-1 possessing an ion crystal structure is not soluble in alkanes. From DRIFTS analysis, after five reuses, the spent HPA-1 catalyst retained the Keggin structure as evidenced by the presence of the

four characteristic infrared bands of HPA-1 in the spectrum (Figure S3). Some adsorbed DBT sulfone was also present on the catalyst surface, as detected by DRIFTS (Figure S3).

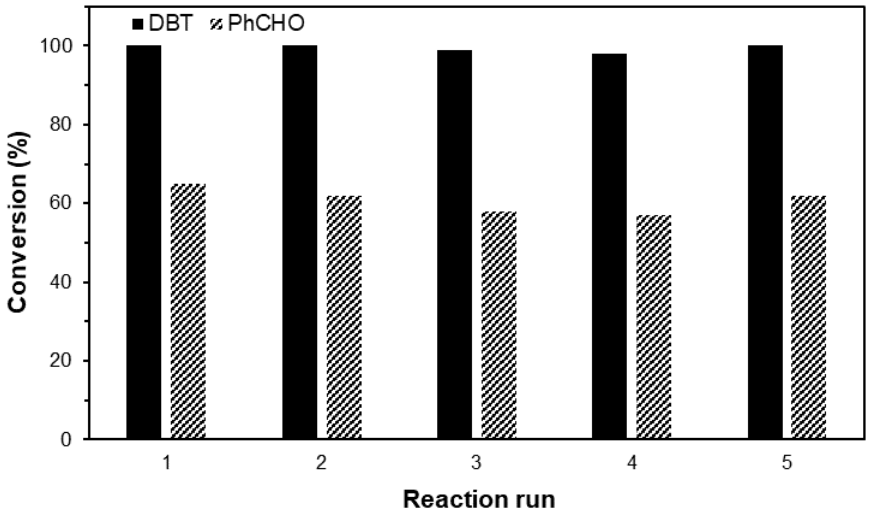

Figure 4. Catalyst reuse for co-oxidation of DBT (0.50 mmol) and PhCHO (3.7 mmol) at 100 °C, HPA-1 (0.10 g, 0.048 mmol), 10 mL dodecane, 1300 rpm stirring speed, 20 mL min^{-1} air flow rate, 2 h reaction time.

Table 3 shows the results on the aldehyde-assisted ODS reaction in the presence of supported HPA-1 catalysts. Silica-supported 15%HPA-1/SiO_2 gave 61% DBT conversion at 100 °C and PhCHO/DBT = 7.4 in a 2 h reaction time; the conversion increased to 80% at 120 °C. The 15%HPA-1/C showed a low activity, giving only 11% DBT conversion in the same conditions. For comparison, bulk HPA-1 in the same conditions and with the same amount of HPA-1 (0.0082 mmol) gave 100% DBT conversion in 1 h (Table 3). Therefore, the supported HPA-1 catalysts were much less efficient than bulk HPA-1. This may be explained by reaction inhibition by the porous supports possessing high surface area; solid surfaces are well known for their efficient radical trapping [28].

Table 3. Aerobic co-oxidation of DBT and PhCHO catalyzed by supported HPA-1 [1].

Catalyst	Temperature (°C)	Conversion (%)	
		DBT	PhCHO
15%HPA-1/SiO_2	100	61	48
15%HPA-1/SiO_2	120	80	53
15%HPA-1/C	100	11	60
Bulk HPA-1 [2]	100	100	69

[1] 0.10 g catalyst (0.0082 mmol HPA-1), 0.50 mmol DBT, 3.7 mmol PhCHO, 10 mL dodecane, 20 mL min^{-1} air flow rate, 1300 rpm stirring speed, 2 h reaction time. [2] Reaction with 0.0082 mmol of bulk HPA-1, 1 h reaction time.

The time course for DBT consumption showed an induction period, whereas no induction period was observed for PhCHO consumption (Figure 5). Previously, an induction period has been observed for O_2 consumption in the DBT/aldehyde co-oxidation catalyzed by $Co(Oac)_2$ in agreement with the radical reaction mechanism [23]. The oxidation of PhCHO, in the presence and in the absence of DBT alike, obeyed the first-order rate law (Figure 6). The oxidation of DBT also followed first-order kinetics after the induction period (Figure 7). For the oxidation of PhCHO, an apparent activation energy (E_a) of 38 kJ mol^{-1} was determined in the temperature range of 40–100 °C (Figure 8). For the oxidation of DBT, the corresponding E_a value determined after the induction period was 66 kJ mol^{-1} (Figure 9).

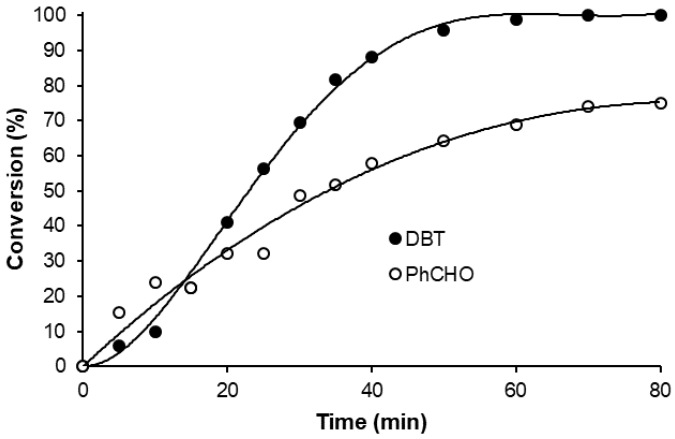

Figure 5. Time course for aerobic co-oxidation of DBT (0.50 mmol) and PhCHO (4.9 mmol) catalyzed by HPA-1 (0.10 g, 0.048 mmol) at 100 °C, 10 mL dodecane, 20 mL min^{-1} air flow and 1300 rpm stirring speed.

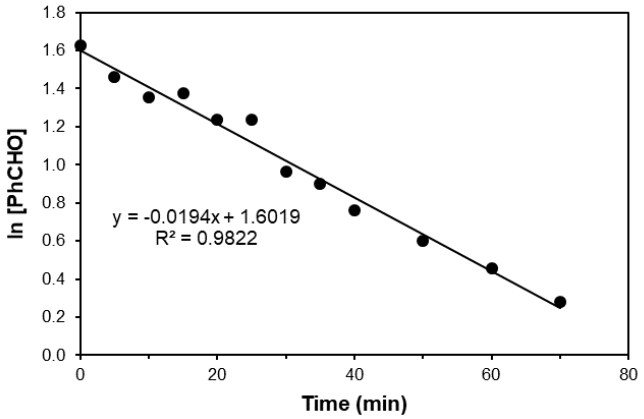

Figure 6. First-order plot $\ln([PhCHO]/[PhCHO]_o) = -k_{ald}\,t$ for aerobic oxidation of PhCHO (4.9 mmol) catalyzed by HPA-1 (0.10 g, 0.048 mmol) at 100 °C, 0.50 mmol DBT, 10 mL dodecane, 20 mL min^{-1} air flow, 1300 rpm stirring speed; k_{ald} = 0.019 min^{-1}.

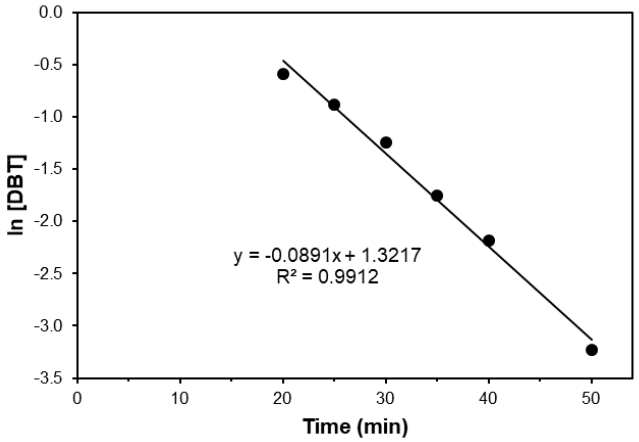

Figure 7. First-order plot after induction period for aerobic oxidation of DBT (0.50 mmol) in the presence of PhCHO (4.9 mmol) catalyzed by HPA-1 (0.10 g, 0.048 mmol) at 100 °C, 10 mL dodecane, 20 mL min^{-1} air flow and 1300 rpm stirring speed; k_{DBT} = 0.089 min^{-1}.

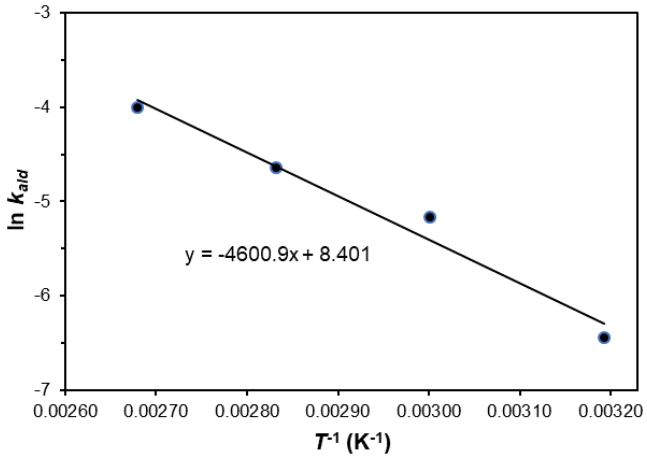

Figure 8. Arrhenius plot for aerobic oxidation of PhCHO (4.9 mmol) catalyzed by HPA-1 (0.10 g, 0.048 mmol) in the presence of DBT (0.50 mmol); 10 mL dodecane, 20 mL min^{-1} air flow and 1300 rpm stirring speed; k_{ald} is the first-order rate constant (min^{-1}); E_a = 38 kJ mol^{-1}.

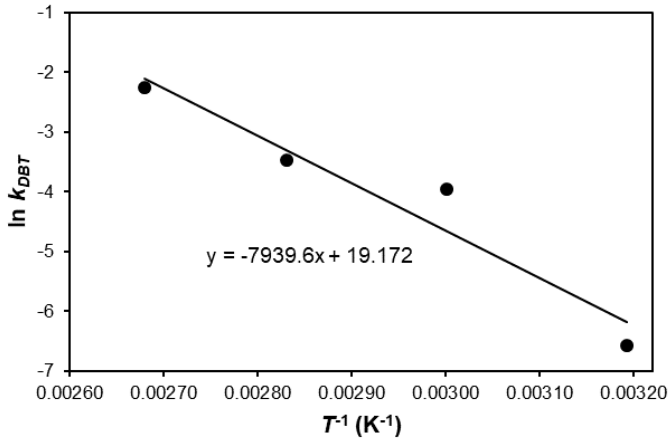

Figure 9. Arrhenius plot for aerobic oxidation of DBT (0.50 mmol) catalyzed by HPA-1 (0.10 g, 0.048 mmol) in the presence of PhCHO (4.9 mmol); 10 mL dodecane, 20 mL min^{-1} air flow and 1300 rpm stirring speed; k_{DBT} is the first-order rate constant (min^{-1}) determined after induction period (see Figure 7); E_a = 66 kJ mol^{-1}.

It is well established that the metal-catalyzed aerobic oxidation (autoxidation) of aldehydes occurs by the radical chain mechanism through peroxy acid intermediates to form the corresponding carboxylic acids as the final products [28]. Organosulfur compounds are well known as inhibitors of radical oxidation by intercepting organic peroxides (Reaction (2)) [28]. Therefore, in the presence of DBT, the peroxy acid will react fast with DBT to form DBT sulfoxide and sulfone [23]. From GC analysis, the products of DBT and PhCHO co-oxidation were DBT sulfone and benzoic acid. Hence, the overall reaction can be represented by Scheme 1.

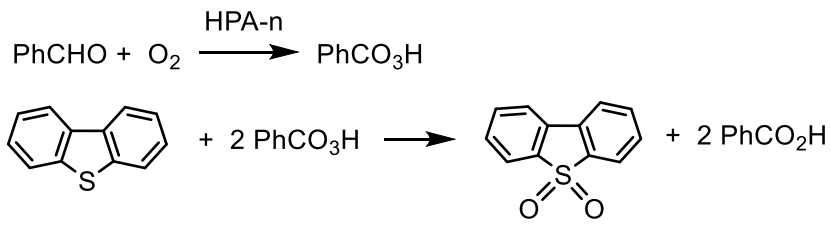

Scheme 1. Aerobic oxidation of DBT in the presence of PhCHO as a sacrificial reductant.

The co-oxidation of PhCHO and DBT by O_2 catalyzed by HPA-1 can be represented by an unbranched radical chain mechanism (Scheme 2). The initiation Step (1) is suggested to involve one-electron oxidation of PhCHO by V^{5+} on the surface of HPA-1 to produce free acyl radical PhCO· and V^{4+}. The catalyst, initially orange, turned green in the reacting mixture, which indicated its reduction. The reduction of V^{5+} to V^{4+} inside HPA-2 by aldehyde has been shown by ESR [37]. The propagation Steps (2)–(3) involve very fast reaction between PhCO· and O_2 to give the acylperoxo radical PhC(O)OO· (Step 2) followed by interaction of PhC(O)OO· with PhCHO to give the peroxy acid PhC(O)OOH and re-form the acyl radical (Step 3) [28]. The acylperoxo radical PhC(O)OO· has been registered in the autoxidation of PhCHO by ESR spin trapping [38]. The acyl radical can decompose to form alkyl radical and CO if there is an O_2 deficiency (O_2 partial pressure <10 kPa) [28], but in our system ($P_{O2} \approx 20$ kPa) this is unlikely. In the absence of DBT, benzoic acid is likely to form by Baeyer–Villiger reaction between the peroxy acid and PhCHO (Step 4) [28]. This is followed by the termination step, involving interaction of the acylperoxo radical with V^{4+} within the HPA-1 heteropoly anion, thus re-oxidizing the catalyst (Step 5). Re-oxidation of V^{4+} by O_2 is unlikely as the oxidation of the reduced HPA-1 by O_2 is difficult in contrast to HPA-n with n = 2–6 [13,31,32]. The oxidation of PhCHO in the presence of bulk HPA-1 can be viewed as a heterogeneous–homogeneous reaction with heterogeneous initiation Step (1) and homogeneous chain-propagating Steps (2)–(3).

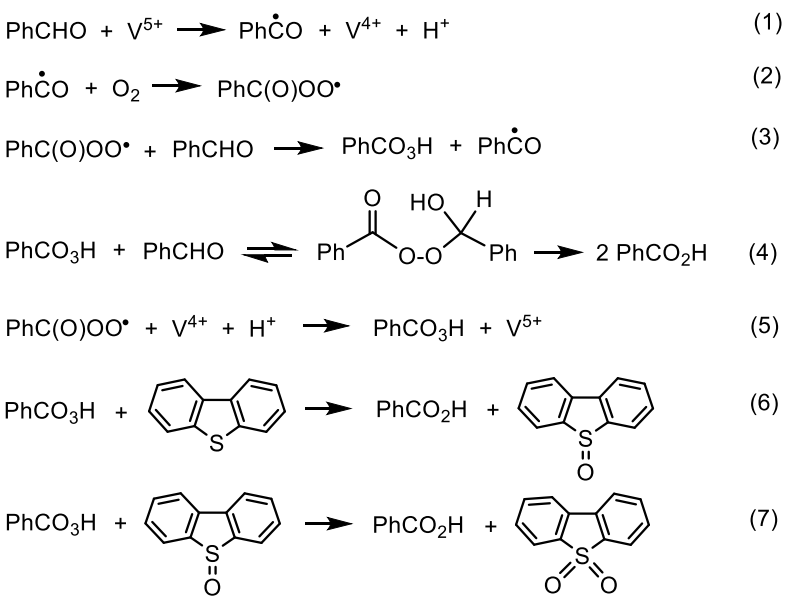

Scheme 2. Proposed mechanism for aerobic co-oxidation of DBT and PhCHO catalyzed by HPA-n.

In the presence of DBT, the peroxy acid reacts further with DBT to form DBT sulfoxide (Step 6) and sulfone (Step 7) [23]. If we assume that PhCHO is mainly consumed in Step (3), i.e., the reaction has a long chain length, and Steps (6) and (7) are faster than (4), then at PhCHO/DBT = 10 mol/mol, the rate of DBT consumption is expected to be five times faster than the rate of PhCHO consumption. This is in good agreement with the observed first-order rate constants for consumption of DBT (k_{DBT} = 0.089 min^{-1}, Figure 6) and PhCHO (k_{ald} = 0.019 min^{-1}, Figure 7)—the former is 4.7 times greater than the latter.

The proposed mechanism is supported by strong inhibition of the ODS reaction by chain-terminating inhibitors (Table 2) (for the mechanism of chain termination, see [28,39]). The induction period in DBT consumption (Figure 5) is also consistent with this mechanism since DBT oxidation follows the oxidation of PhCHO in a consecutive process. Therefore, the proposed unbranched radical chain mechanism for the aldehyde-assisted aerobic ODS reaction catalyzed by HPA-n is in good compliance with the experimental data. Similar radical mechanisms have been suggested for aerobic co-oxidation of alkanes [37] and alkenes [40] with aldehydes catalyzed by HPA-n.

3. Materials and Methods

3.1. Chemicals and Catalysts

Dibenzothiophene (99%, DBT), dodecane (99%), 30% H_2O_2, $H_3PMo_{12}O_{40}$ hydrate (99.9%), 1,4-benzoquinone (96%), 2,6-di-tert-butyl-4-methylphenol (99%) and Darco KB-B activated carbon (wet powder, 150 μm particle size) were purchased from Sigma-Aldrich (St. Louis, MO, USA). Aerosil 300 silica support was from Degussa.

P–Mo–V heteropoly acids $H_{3+n}PMo_{12-n}V_nO_{40}$ (HPA-n, n = 1–3) were prepared by the established procedure [35] involving interaction of stoichiometric amounts of Na_2MoO_4, $NaVO_3$ and Na_2HPO_4 in aqueous solution followed by extraction of HPA-n from acidified solution with ether, decomposition of HPA-n etherate and crystallization of HPA-n. The samples thus prepared were dried in an oven at 100 °C to afford HPA-n as an orange powder which was then ground to a 45–180 μm particle size. The composition of HPA-n was confirmed by inductively coupled plasma–optical emission spectroscopy (ICP–OES). $Cs_{1.5}H_{2.5}PMo_{11}V_{40}$ (Cs-HPA-1) and $Na_2H_3PMo_{10}V_2O_{40}$ (Na-HPA-2) acidic salts were prepared by partial neutralization of HPA-1 with Cs_2CO_3 and HPA-2 with Na_2CO_3, respectively, in aqueous solution followed by rotary evaporation and drying as above. Silica-supported catalyst 15%HPA-1/SiO_2 was prepared by wet impregnation of Aerosil 300 silica powder with an aqueous solution of HPA-1 followed by rotary evaporation of water. The catalyst was vacuum dried at 150 °C/1 Pa for 1.5 h and finally ground to a 45–180 μm particle size. Carbon-supported catalyst 15%HPA-1/C was prepared by impregnating HPA-1 onto Darco KB-B activated carbon from aqueous solution as described elsewhere [41] and air dried in an oven at 100 °C.

3.2. Catalyst Characterization

Brunauer–Emmett–Teller (BET) analysis of catalyst samples was performed on a Micrometrics ASAP 2010 instrument by measuring N_2 physisorption at –196 °C. The samples were pre-treated at 150 °C under vacuum (1 Pa). Diffuse reflectance infrared Fourier transform (DRIFT) spectra were recorded on a Nicolet Nexus FTIR spectrometer using powdered catalyst mixtures with KBr. The spectra were recorded at room temperature by averaging 254 scans in the range of 4000–500 cm^{-1} with a resolution of 4 cm^{-1}. Powder X-ray diffraction (XRD) patterns of catalysts were recorded on a PANalytical Xpert diffractometer with CuKα radiation (λ = 1.542 Å). Thermogravimetric analysis (TGA) was carried out on a Perkin Elmer TGA-7 instrument under N_2 flow. The chemical composition of HPA-n, 15%HPA-1/C and 15%HPA-1/SiO_2 was determined on a Spectro Ciros ICP–OES analyzer; the samples were digested by boiling in aqueous 15% KOH. Information about the catalysts prepared is shown in Table 1.

3.3. Reaction Procedure

The aerobic co-oxidation of DBT (0.4–0.5 mmol) and PhCHO (0–5.9 mmol) in the presence of powdered HPA-n catalysts (ca. 1 wt% per total reaction mixture) was carried out in dodecane as a solvent (10 mL) at 40–120 °C in a 50 mL semi-batch jacketed glass reactor equipped with a heat circulator, a magnetic stirrer, a reflux condenser and an air inlet. Tetradecane (0.40 mmol) was added to the reaction mixture as an internal GC standard. During reaction, air was bubbled through the reaction mixture at a flow rate of 20 mL min^{-1}, unless stated otherwise. The reaction was carried out at 1300 rpm stirring speed. Reaction rate did not depend on the stirring speed in the range of 300–1500 rpm, which indicated no external diffusion limitation and sufficient oxygen supply. DBT conversion was monitored by submitting aliquots of reaction mixture (0.1 mL, centrifuged to separate the catalyst) for GC analysis (a Varian Chrompack CP-3380 gas chromatograph equipped with a flame ionization detector and a 25 m × 0.32 mm × 0.5 μm BP1 capillary column). Every reaction was repeated at least twice with a good reproducibility. Generally, the mean absolute percentage error in DBT and PhCHO conversion was ≤5%.

For catalyst reuse, the initial reaction was run for 2 h. The catalyst was separated using a centrifuge, washed with toluene to remove DBT sulfone and then washed with

dodecane in a centrifuge tube. After that, the catalyst was returned to the reactor along with the required amounts of all other reaction components for the next run.

4. Conclusions

Aerobic ODS of model liquid fuel (dodecane spiked with DBT) occurs readily at ambient air pressure in the presence of bulk heteropoly acid $H_4PMo_{11}VO_{40}$ (HPA-1) as a heterogeneous catalyst and benzaldehyde as a sacrificial reductant. It removes 100% of DBT from fuel (converted to DBT sulfone) in 2 h either at 60 °C and PhCHO/DBT = 12 mol/mol or at 100 °C and PhCHO/DBT = 5.6. The catalyst can be recycled without loss of activity. The ODS reaction is suggested to occur through an unbranched radical chain mechanism. It can be viewed as a heterogeneous–homogeneous reaction with a heterogeneous initiation step and homogeneous chain-propagating steps.

Supplementary Materials: The following are available online at https://www.mdpi.com/article/10.3390/catal11080988/s1, Figure S1: DRIFT spectrum (in KBr) of 15%HPA-1/C and bulk HPA-1; Figure S2. DRIFT spectra (in KBr): 15%HPA-1/SiO2 (1) and bulk HPA-1 (2). Bands at 476 and 1101 cm^{-1} belong to silica support. The presence of bands at 786, 866 and 964 cm^{-1} in spectrum (1) confirms that the Keggin structure of HPA-1 is intact in 15%HPA-1/SiO_2; Figure S3. DRIFT spectra (in KBr) of fresh and spent HPA-1 catalyst after 5 successive runs: fresh HPA-1 (1), spent HPA-1 catalyst after 5 successive runs (2) and DBT sulfone (3).

Author Contributions: Conceptualization, I.V.K. and R.Y.; methodology, I.V.K. and E.F.K.; investigation, R.G. and R.H.; data curation, R.G. and R.H.; writing—original draft preparation, R.G.; writing—review and editing, I.V.K.; supervision, I.V.K. and E.F.K. All authors have read and agreed to the published version of the manuscript.

Funding: This research received no external funding.

Acknowledgments: We thank Jazan University, Jazan, Saudi Arabia, for Ph.D. scholarship for R.G.

Conflicts of Interest: The authors declare no conflict of interest.

References

1. Babich, I.V.; Moulijn, J.A. Science and technology of novel processes for deep desulfurization of oil refinery streams. *Fuel* **2003**, *82*, 607–631. [CrossRef]
2. Prins, R. Hydrotreating. In *Handbook of Heterogeneous Catalysis*; Ertl, G., Knözinger, H., Schüth, F., Weitkamp, J., Eds.; Wiley-VCH: Hoboken, NJ, USA, 2008; Volume 6, pp. 2695–2718.
3. Saha, B.; Vedachalam, S.; Dalai, A.K. Review on recent advances in adsorptive desulfurization. *Fuel Process. Technol.* **2021**, *214*, 106685. [CrossRef]
4. Bhutto, A.W.; Abro, R.; Gao, S.; Abbas, T.; Chen, X.; Yu, G. Oxidative desulfurization of fuel oils using ionic liquids: A review. *J. Taiwan Inst. Chem. Eng.* **2016**, *62*, 84–97. [CrossRef]
5. Jiang, Z.; Lü, H.; Zhang, Y.; Li, C. Oxidative desulfurization of fuel oils. *Chin. J. Catal.* **2011**, *32*, 707–715. [CrossRef]
6. Eseva, E.A.; Akopyan, A.V.; Anisimov, A.V.; Maksimov, A.L. Oxidative desulfurization of hydrocarbon feedstock using oxygen as oxidizing agent (a review). *Petroleum Chem.* **2020**, *60*, 979–990. [CrossRef]
7. Zhang, Y.; Wang, R. Recent advances on catalysts and systems for the oxidation of thiophene derivatives in fuel oil with molecular oxygen. *Mini Rev. Org. Chem.* **2018**, *15*, 488–497. [CrossRef]
8. Collins, F.M.; Lucy, A.R.; Sharp, C. Oxidative desulphurisation of oils via hydrogen peroxide and heteropolyanion catalysis. *J. Mol. Catal. A* **1997**, *117*, 397–403. [CrossRef]
9. Komintarachat, C.; Trakarnpruk, C. Oxidative desulfurization using polyoxometalates. *Ind. Eng. Chem. Res.* **2006**, *45*, 1853–1856. [CrossRef]
10. Shojaei, A.F.; Rezvani, M.A.; Loghmani, M.H. Comparative study on oxidation desulphurization of actual gas oil and model sulfur compounds with hydrogen peroxide promoted by formic acid: Synthesis and characterization of vanadium containing polyoxometalate supported on anatase crushed nanoleaf. *Fuel Process. Technol.* **2014**, *118*, 1–6. [CrossRef]
11. Mirante, F.; Dias, L.; Silva, M.; Ribeiro, S.O.; Corvo, M.C.; de Castro, B.; Granadeiro, C.M.; Balula, S.S. Efficient heterogeneous polyoxometalate-hybrid catalysts for the oxidative desulfurization of fuels. *Catal. Commun.* **2018**, *104*, 1–8. [CrossRef]
12. Craven, M.; Yahya, R.; Kozhevnikova, E.F.; Robertson, C.M.; Steiner, A.; Kozhevnikov, I.V. Alkylaminophosphazenes as efficient and tuneable phase-transfer agents for polyoxometalate-catalyzed biphasic oxidation with hydrogen peroxide. *ChemCatChem* **2016**, *8*, 200–208. [CrossRef]
13. Kozhevnikov, I.V. *Catalysts for Fine Chemical Synthesis: Catalysis by Polyoxometalates*; Wiley: West Sussex, UK, 2002.

14. Li, J.; Yang, Z.; Li, S.; Jin, Q.; Zhao, J. Review on oxidative desulfurization of fuel by supported heteropolyacid catalysts. *J. Ind. Eng. Chem.* **2020**, *82*, 1–16. [CrossRef]
15. Taghizadeh, M.; Mehrvarz, E.; Taghipour, A. Polyoxometalate as an effective catalyst for the oxidative desulfurization of liquid fuels: A critical review. *Rev. Chem. Eng.* **2020**, *36*, 831–858. [CrossRef]
16. Xu, J.; Zhu, Z.; Su, T.; Liao, T.; Deng, C.; Hao, D.; Zhao, Y.; Ren, W.; Lü, H. Green aerobic oxidative desulfurization of diesel by constructing an Fe-Anderson type polyoxometalate and benzene sulfonic acid-based deep eutectic solvent biomimetic cycle. *Chin. J. Catal.* **2020**, *41*, 868–876. [CrossRef]
17. Tang, N.; Zhang, Y.; Lin, F.; Lu, H.; Jiang, Z.; Li, C. Oxidation of dibenzothiophene catalyzed by $[C_8H_{17}N(CH_3)_3]_3H_3V_{10}O_{28}$ using molecular oxygen as oxidant. *Chem. Commun.* **2012**, *48*, 11647–11649. [CrossRef] [PubMed]
18. Li, J.K.; Xu, Y.Q.; Hu, C.W. In Situ synthesis of a novel dioxidovanadium-based nickel complex as catalyst for deep oxidative desulfurization with molecular oxygen. *Inorg. Chem. Commun.* **2015**, *60*, 12–14. [CrossRef]
19. Zhang, M.; Liu, J.; Li, H.; Wei, Y.; Fu, Y.; Liao, W.; Zhu, L.; Chen, G.; Zhu, W.; Li, H. Tuning the electrophilicity of vanadium-substituted polyoxometalate based ionic liquids for high-efficiency aerobic oxidative desulfurization. *Appl. Catal. B* **2020**, *271*, 118936. [CrossRef]
20. Claußnitzer, J.; Bertleff, B.; Korth, W.; Albert, J.; Wasserscheid, P.; Jess, A. Kinetics of triphase extractive oxidative desulfurization of benzothiophene with molecular oxygen catalyzed by HPA-5. *Chem. Eng. Technol.* **2020**, *43*, 465–475. [CrossRef]
21. Wang, R.; Zhao, Y.; Kozhevnikov, I.V.; Zhao, J. An ultrasound enhanced catalytic ozonation process for the ultra-deep desulfurization of diesel oil. *New J. Chem.* **2020**, *44*, 15467–15474. [CrossRef]
22. Pope, M.T. *Heteropoly and Isopoly Oxometalates*; Springer: Berlin/Heidelberg, Germany, 1983.
23. Murata, S.; Murata, K.; Kidena, K.; Nomura, M. A novel oxidative desulfurization system for diesel fuels with molecular oxygen in the presence of cobalt catalysts and aldehydes. *Energy Fuels* **2004**, *18*, 116–121. [CrossRef]
24. Lu, H.; Gao, J.; Jiang, Z.; Yang, Y.; Song, B.; Li, C. Oxidative desulfurization of dibenzothiophene with molecular oxygen using emulsion catalysis. *Chem. Commun.* **2007**, 150–152. [CrossRef] [PubMed]
25. Dumont, V.; Oliviero, L.; Mauge, F.; Houalla, M. Oxidation of dibenzothiophene by a metal–oxygen–aldehyde system. *Catal. Today* **2008**, *130*, 195–198. [CrossRef]
26. Rao, T.V.; Krishna, P.M.; Paul, D.; Nautiyal, B.R.; Kumar, J.; Sharma, Y.K.; Nanoti, S.M.; Sain, B.; Garg, M.O. The oxidative desulfurization of HDS diesel: Using aldehyde and molecular oxygen in the presence of cobalt catalysts. *Petrol. Sci. Technol.* **2011**, *29*, 626–632. [CrossRef]
27. Wang, C.; Chen, Z.; Zhu, W.; Wu, P.; Jiang, W.; Zhang, M.; Li, H.; Zhu, W.; Li, H. One-pot extraction and oxidative desulfurization of fuels with molecular oxygen in low-cost metal-based ionic liquids. *Energy Fuels* **2017**, *31*, 1376–1382. [CrossRef]
28. Teles, J.H.; Hermans, I.; Franz, G.; Sheldon, R.A. *Oxidation, Ullmann's Encyclopedia of Industrial Chemistry*; Wiley–VCH: Weinheim, Germany, 2015.
29. Weissermel, K.; Arpe, H.J. *Industrial Organic Chemistry*, 4th ed.; Wiley–VCH: Weinheim, Germany, 2003.
30. Li, J.; Chu, X.; Tian, S. Research on determination of total acid number of petroleum using mid-infrared attenuated total reflection spectroscopy. *Energy Fuels* **2012**, *26*, 5633–5637.
31. Kozhevnikov, I.V.; Matveev, K.I. Homogeneous catalysts based on heteropoly acids. *Appl. Catal.* **1983**, *5*, 135–150. [CrossRef]
32. Kozhevnikov, I.V. Catalysis by heteropoly acids and multicomponent polyoxometalates in liquid-phase reactions. *Chem. Rev.* **1998**, *98*, 171–198. [CrossRef] [PubMed]
33. Weinstock, I.A.; Schreiber, R.E.; Neumann, R. Dioxygen in polyoxometalate mediated reactions. *Chem. Rev.* **2018**, *118*, 2680–2717. [CrossRef]
34. Tong, J.; Wang, W.; Su, L.; Li, Q.; Liu, F.; Ma, W.; Lei, Z.; Bo, L. Highly selective oxidation of cyclohexene to 2-cyclohexene-1-one over polyoxometalate/metal–organic framework hybrids with greatly improved performances. *Catal. Sci. Technol.* **2017**, *7*, 222–230. [CrossRef]
35. Tsigdinos, G.A.; Hallada, C.J. Molybdovanadophosphoric acids and their salts. 1. Investigation of methods of preparation and characterization. *Inorg. Chem.* **1968**, *7*, 437–441. [CrossRef]
36. Kanno, M.; Yasukawa, T.; Ninomiya, W.; Ooyachi, K.; Kamiya, Y. Catalytic oxidation of methacrolein to methacrylic acid over silica-supported 11-molybdo-1-vanadophosphoric acid with different heteropolyacid loadings. *J. Catal.* **2010**, *273*, 1–8. [CrossRef]
37. Khenkin, A.M.; Rosenberger, A.; Neumann, R. Reaction of aldehydes with the $H_5PV_2Mo_{10}O_{40}$ polyoxometalate and co-oxidation of alkanes with molecular oxygen. *J. Catal.* **1999**, *182*, 82–91. [CrossRef]
38. Sankar, M.M.; Nowicka, E.; Carter, E.; Murphy, D.M.; Knight, D.M.; Bethell, D.; Hutchings, G.J. The benzaldehyde oxidation paradox explained by the interception of peroxy radical by benzyl alcohol. *Nat. Commun.* **2014**, *5*, 3332. [CrossRef] [PubMed]
39. Ingold, K.U.; Pratt, D.A. Advances in radical-trapping antioxidant chemistry in the 21st century: A kinetics and mechanisms perspective. *Chem. Rev.* **2014**, *114*, 9022–9046. [CrossRef] [PubMed]
40. Hamamoto, M.; Nakayama, K.; Nishiyama, Y.; Ishii, Y. Oxidation of organic substrates by molecular oxygen/aldehyde/heteropolyoxometalate system. *J. Org. Chem.* **1993**, *58*, 6421–6425. [CrossRef]
41. Ghubayra, R.; Nuttall, C.; Hodgkiss, S.; Craven, M.; Kozhevnikova, E.F.; Kozhevnikov, I.V. Oxidative desulfurization of model diesel fuel catalyzed by carbon-supported heteropoly acids. *Appl. Catal. B* **2019**, *253*, 309–316. [CrossRef]